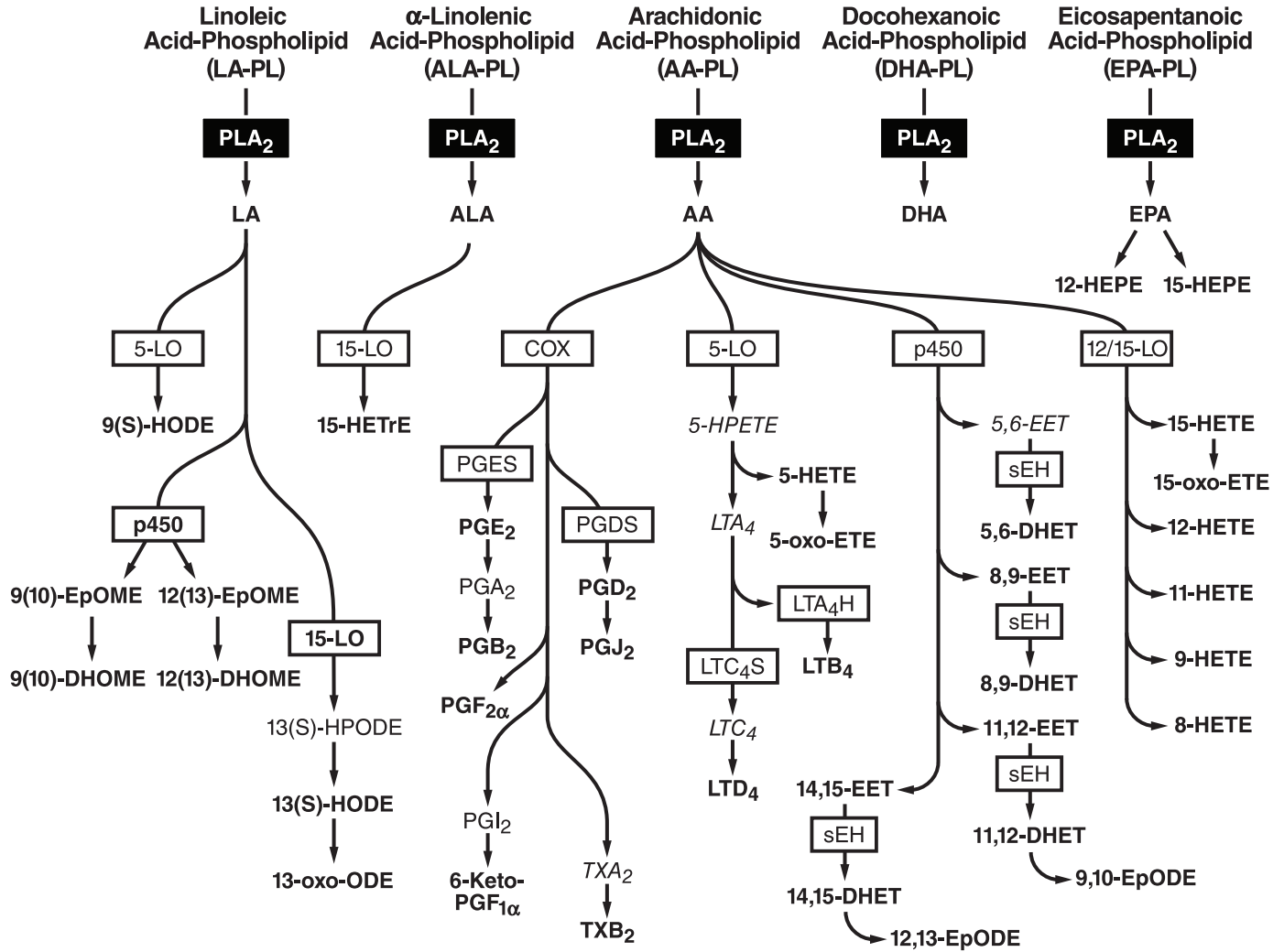
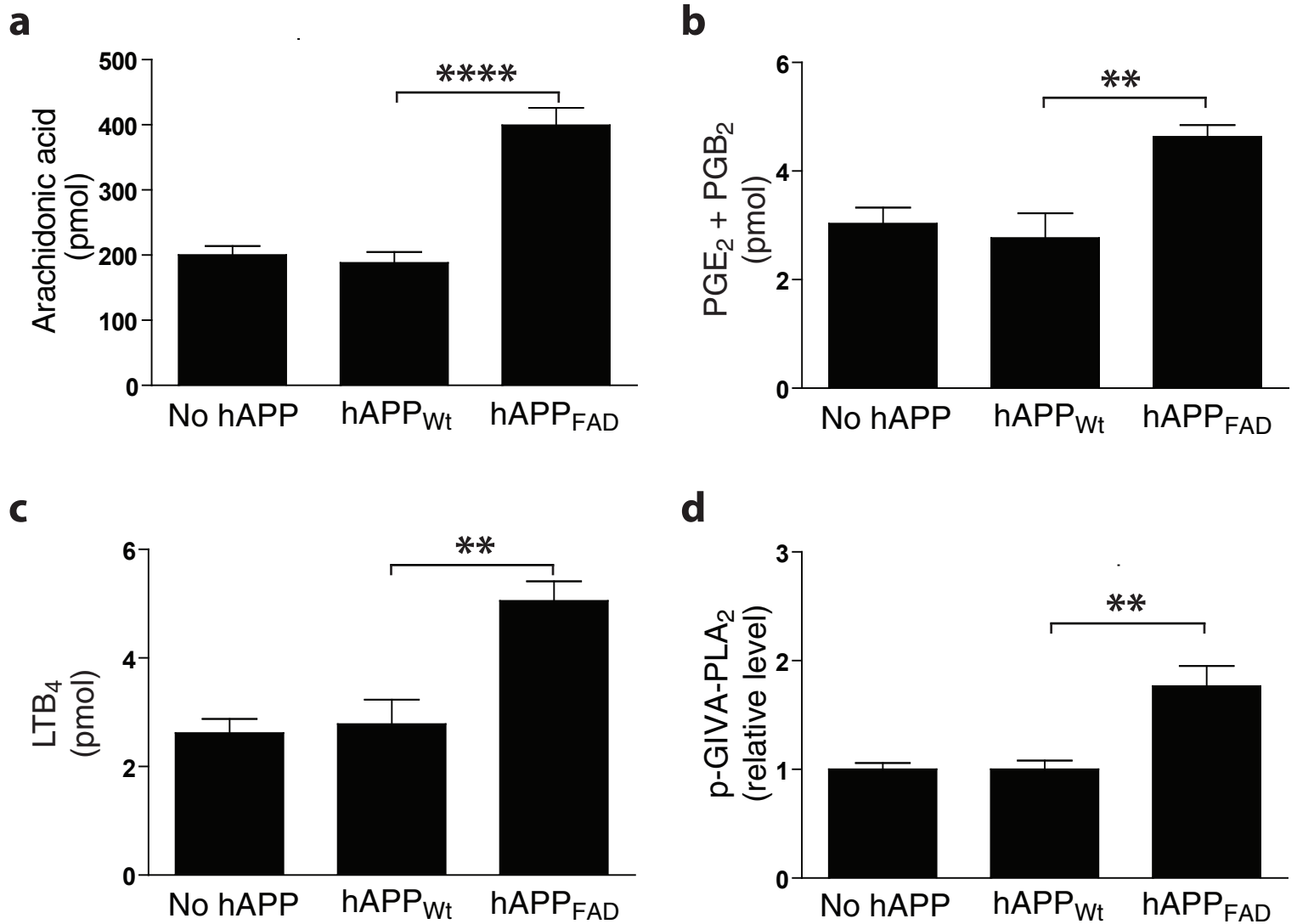


## Supplementary Figure 1



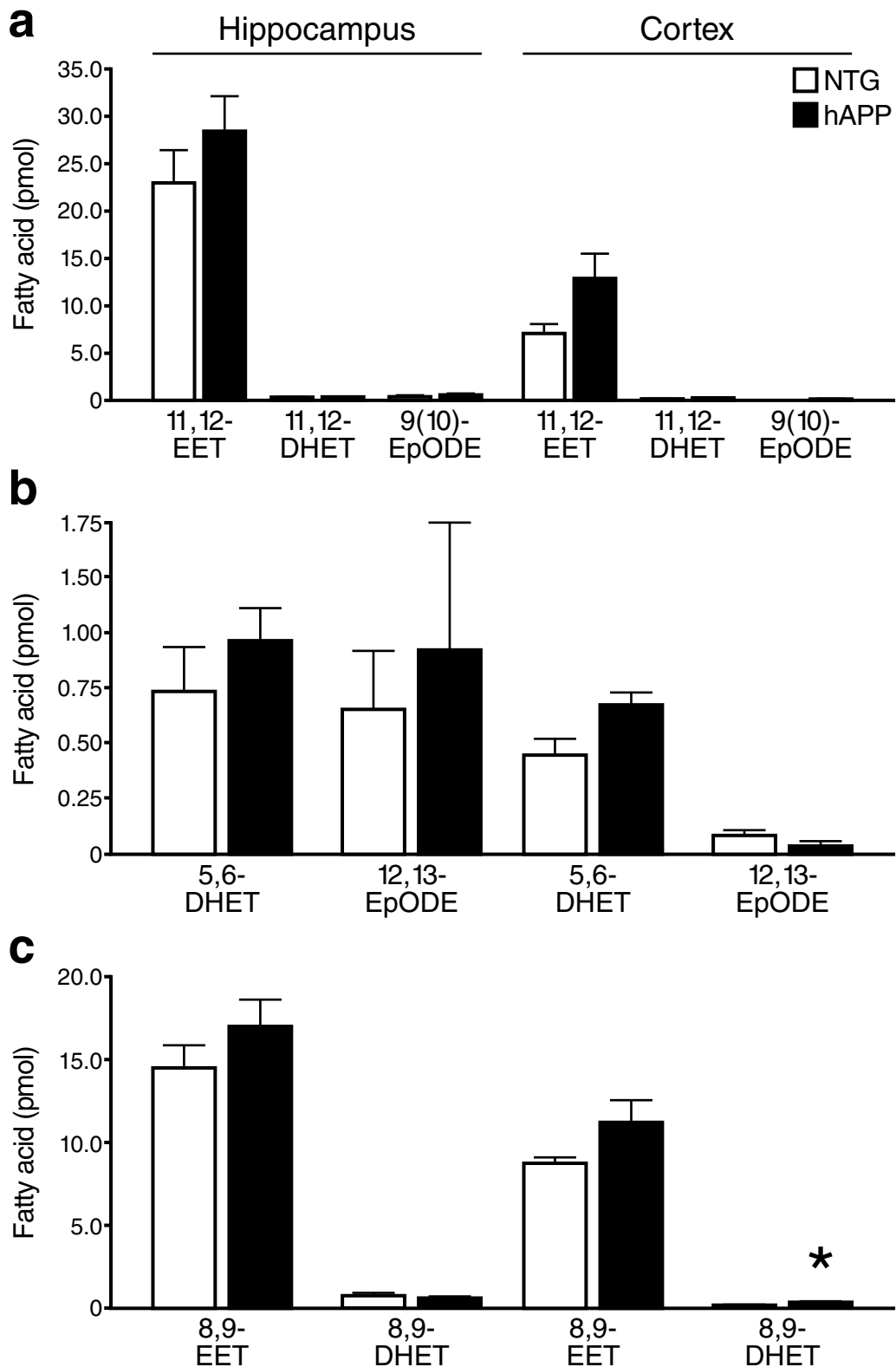
**Supplementary Figure 1.** PLA<sub>2</sub>-dependent fatty acid metabolism. PLA<sub>2</sub> mediates the release of fatty acids from membrane phospholipids (PL), including linoleic acid (LA), α-linolenic acid (ALA), arachidonic acid (AA), docosahexaenoic acid (DHA), and eicosapentaenoic acid (EPA). These metabolites can be metabolized further by lipoxygenase (LO), cyclooxygenase (COX), or p450 enzymes. LA is metabolized into hydroxyperoxyoctadecadienoic acids (HPODE), hydroxyoctadecadienoic acid (HODE), epoxy-hydroxy-octadecenoic acids (EpOME), epoxyperoxyoctadecadienoic acids (EpODE), dihydroxy-octadecenoic acids (DHOME), and oxo-octadecadienoic acids (oxo-ODE). ALA is metabolized by 15-LO to 15-hydroxyeicosatrienoic acid (HETrE). AA is metabolized into PGs, LTs, EETs, and HETEs. EPA can be metabolized into 12- and 15-hydroxyeicosapentaenoic acid (HEPE). sEH, soluble epoxide hydrolase; LTC<sub>4</sub>S, LTC<sub>4</sub> synthase; LTA<sub>4</sub>H, LTA<sub>4</sub> hydrolase; PGES, PGE<sub>2</sub> synthase; PGDS, PGD<sub>2</sub> synthase. Metabolites measured in this study are highlighted in bold.

## Supplementary Figure 2



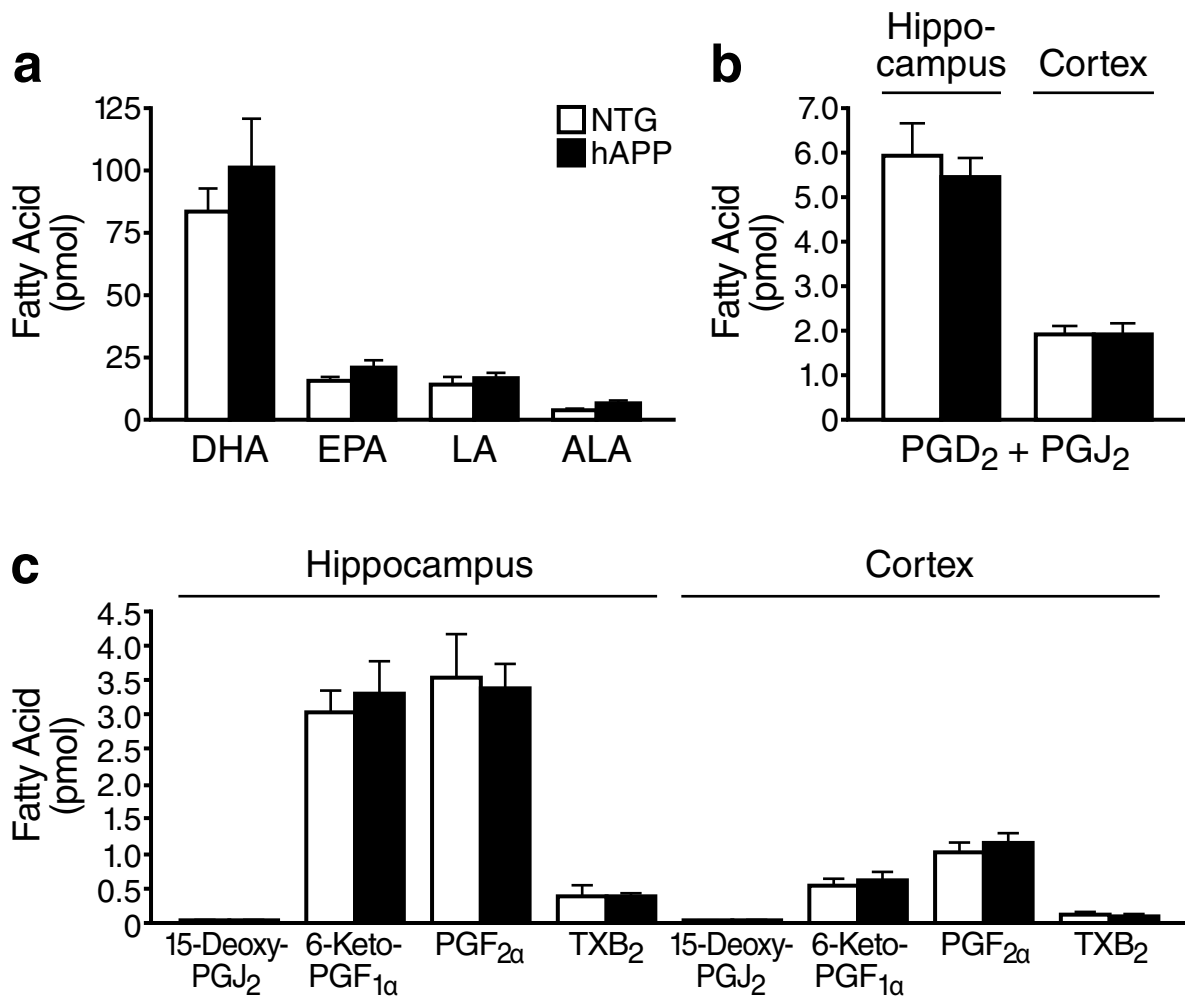
**Supplementary Figure 2.** No change in GIVA-PLA<sub>2</sub>-liberated fatty acids and GIVA-PLA<sub>2</sub> activation in TG mice overexpressing wildtype hAPP. **(a–c)** Levels of AA ( $P < 0.0001$  by one-way ANOVA), PGE<sub>2</sub> + PGB<sub>2</sub> ( $P < 0.01$  by one-way ANOVA), and LTB<sub>4</sub> ( $P < 0.001$  by one-way ANOVA) in 4-month-old NTG, hAPP<sub>WT</sub> TG mice (line I5) and hAPP<sub>FAD</sub> TG mice (line J20). **d**, Phosphorylated-GIVA-PLA<sub>2</sub> levels normalized to tubulin levels in 4-month-old NTG, hAPP<sub>WT</sub> mice and hAPP<sub>FAD</sub> mice ( $P < 0.001$  by one-way ANOVA). \*\* $P < 0.01$ , \*\*\* $P < 0.001$ , \*\*\*\* $P < 0.0001$  by post-hoc Tukey test. Fatty acid levels normalized to mg of total protein in sample.  $n = 6$  mice per genotype (mean  $\pm$  s.e.m.).

Supplementary Figure 3



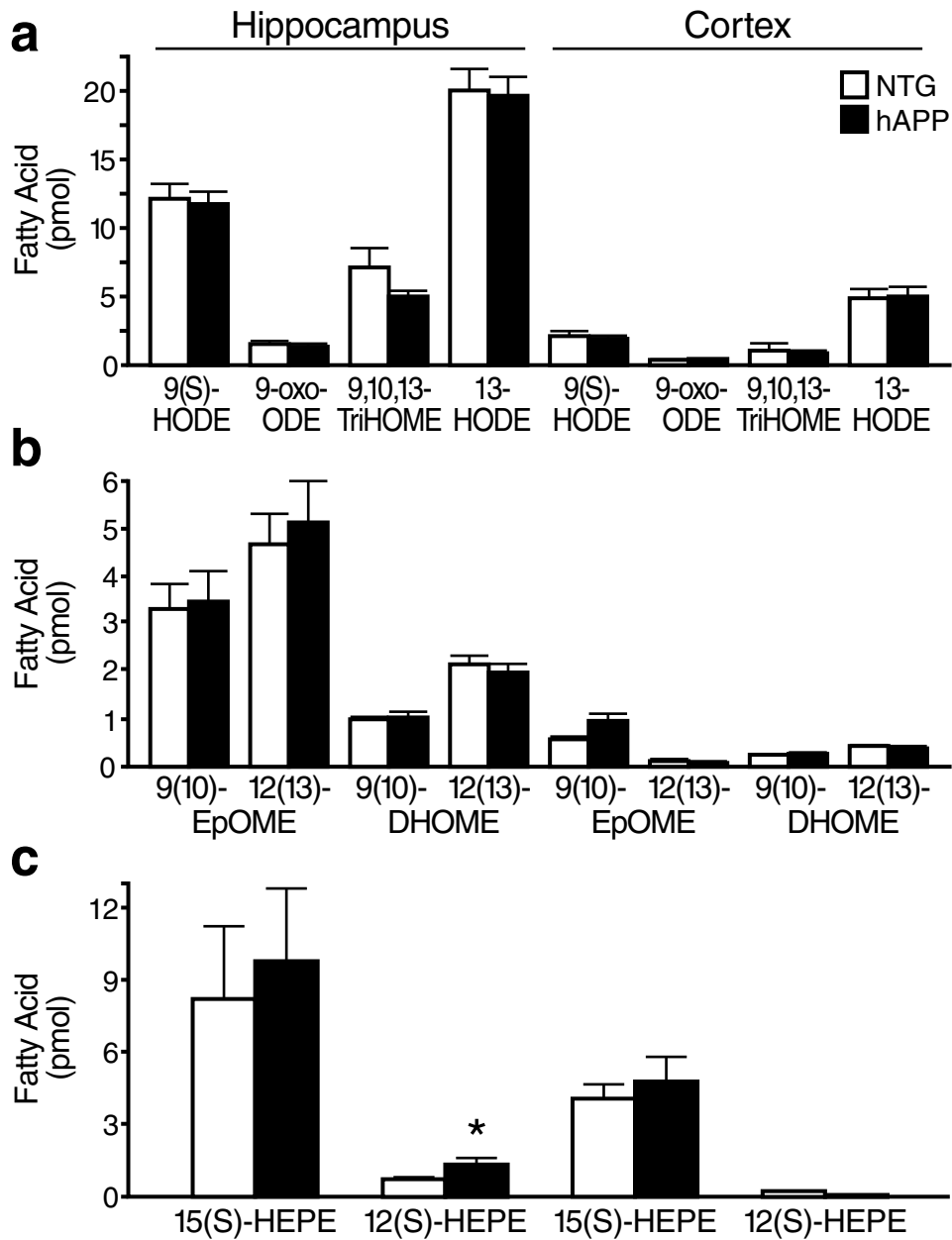
**Supplementary Figure 3.** Levels of EETs and their metabolites in hAPP and NTG mice. (a–c) EETs and their metabolites in the hippocampus and cortex of 4-month-old hAPP<sub>FAD</sub> and NTG mice were measured by simultaneous liquid chromatography-tandem triple quad mass spectrometry. \* $P < 0.05$  by unpaired  $t$  test. Fatty acid levels normalized to mg of total protein in sample.  $n = 12$  mice per genotype (mean  $\pm$  s.e.m.).

Supplementary Figure 4



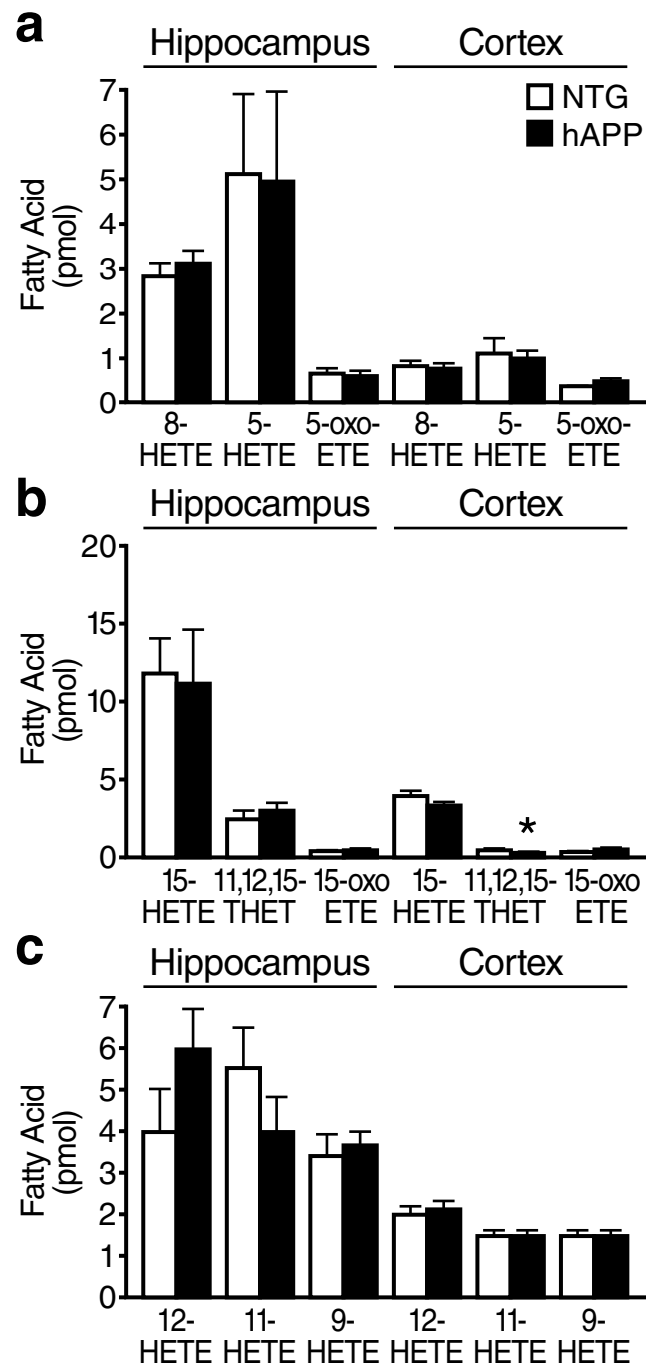
**Supplementary Figure 4.** PLA<sub>2</sub>-liberated fatty acids and prostaglandins in hAPP and NTG mice. PLA<sub>2</sub>-liberated fatty acids (**a**) and prostaglandins (**b**, **c**) in the hippocampus and cortex of 4-month-old hAPP<sub>FAD</sub> and NTG mice were measured by simultaneous liquid chromatography-tandem triple quad mass spectrometry. Fatty acid levels normalized to mg of total protein in sample. n=12 mice per genotype (mean ± s.e.m.).

Supplementary Figure 5

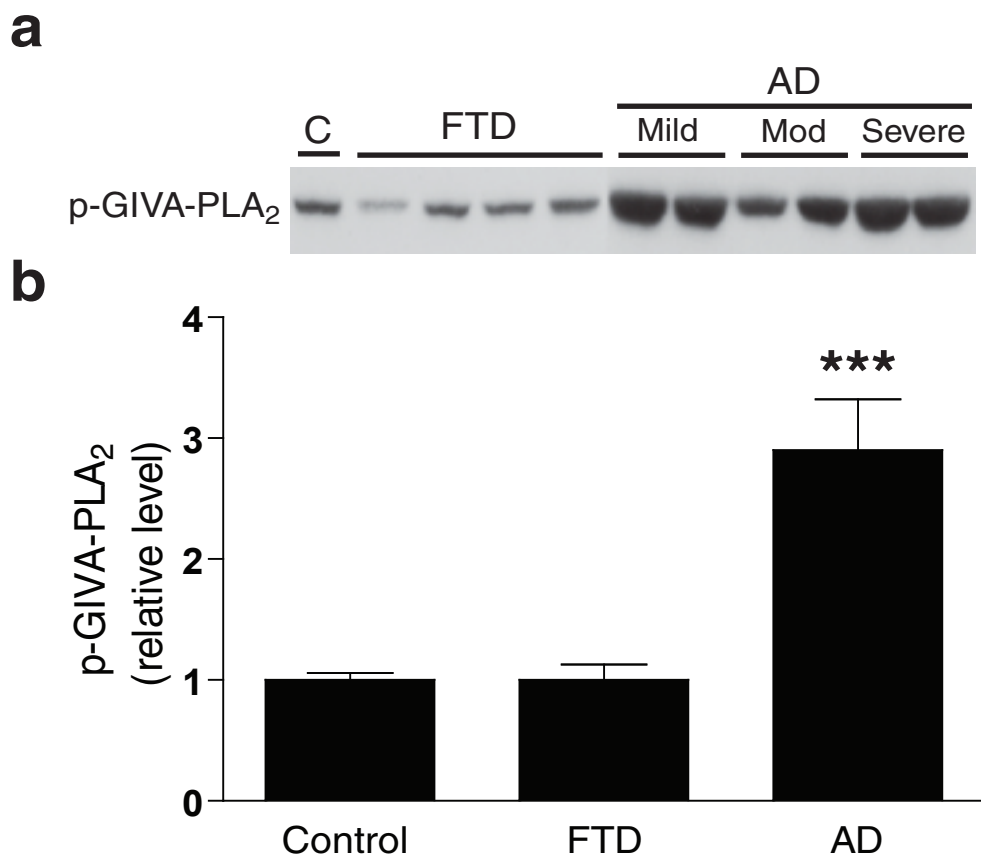


**Supplementary Figure 5.** Levels of LA and EPA metabolites in hAPP and NTG mice. LA (**a**, **b**) and EPA (**c**) metabolites in the hippocampus and cortex of 4-month-old hAPP<sub>FAD</sub> and NTG mice were measured by simultaneous liquid chromatography-tandem triple quad mass spectrometry. \* $P < 0.05$  vs. NTG by unpaired  $t$  test. Fatty acid levels normalized to mg of total protein in sample.  $n = 12$  mice per genotype (mean  $\pm$  s.e.m.).

Supplementary Figure 6

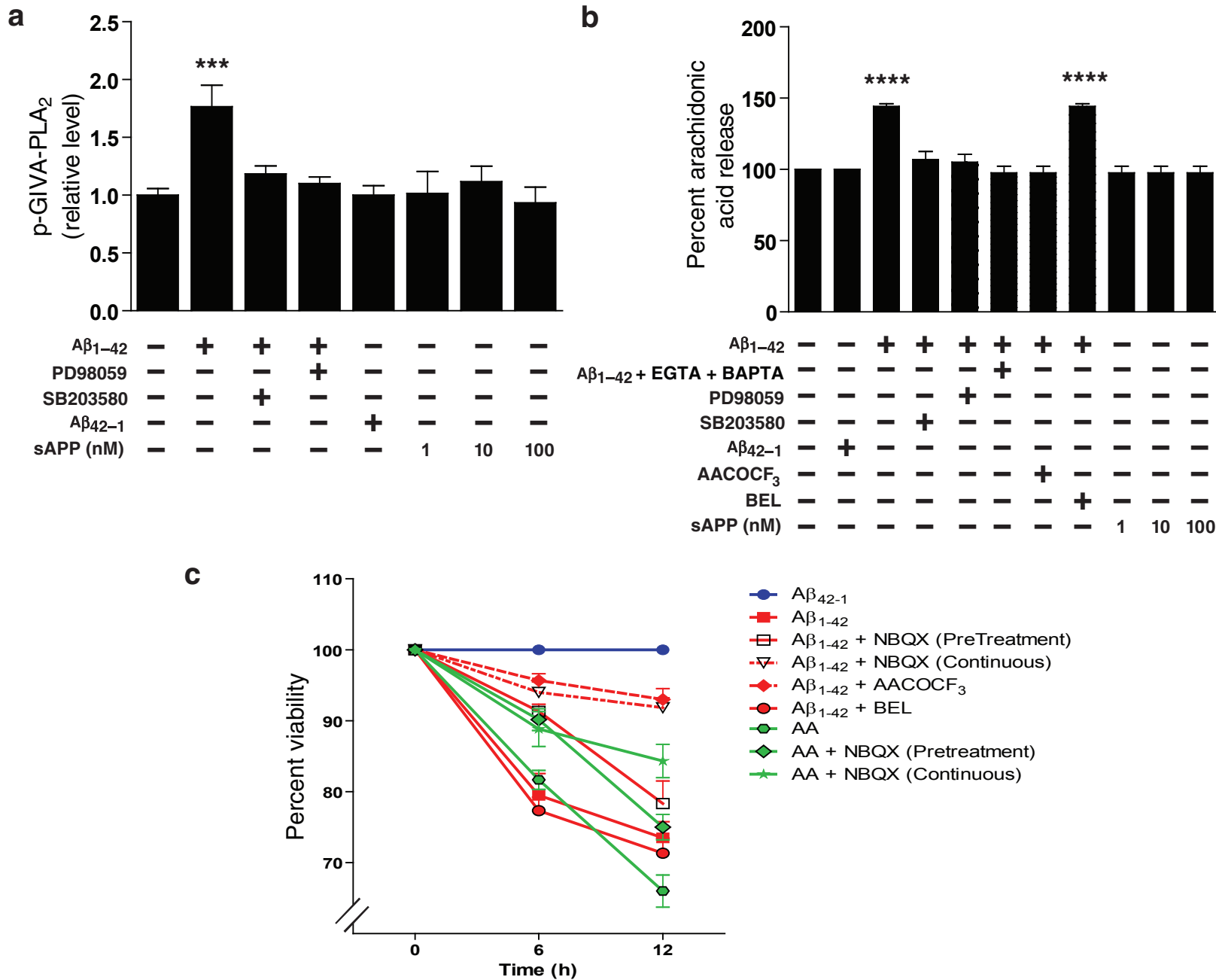


**Supplementary Figure 6.** Levels of HETE metabolites in hAPP and NTG mice. HETE metabolites (**a-c**) in the hippocampus and cortex of 4-month-old hAPP<sub>FAD</sub> and NTG mice were measured by simultaneous liquid chromatography-tandem triple quad mass spectrometry. \* $P < 0.05$  vs. NTG by unpaired  $t$  test. Fatty acid levels normalized to mg of total protein in sample.  $n = 12$  mice per genotype (mean  $\pm$  s.e.m.).



**Supplementary Figure 7.** Levels of phosphorylated GIVA-PLA<sub>2</sub> in AD and controls. **a**, Western blot analysis of hippocampal *postmortem* tissues from AD patients, age-matched non-demented controls, and FTD patients with an antibody that specifically recognizes phosphorylated (p) GIVA-PLA<sub>2</sub>. **b**, Levels of p-GIVA-PLA<sub>2</sub> were higher in AD patients compared to age-matched non-demented controls and FTD patients (P<0.001 by one-way ANOVA). \*\*\*P<0.001 vs. control groups by post-hoc Tukey test. p-GIVA-PLA<sub>2</sub> levels were normalized to tubulin levels. n=12 for AD patients, n=6 for non-demented controls, and n=4 for FTD patients (mean ± s.e.m.).

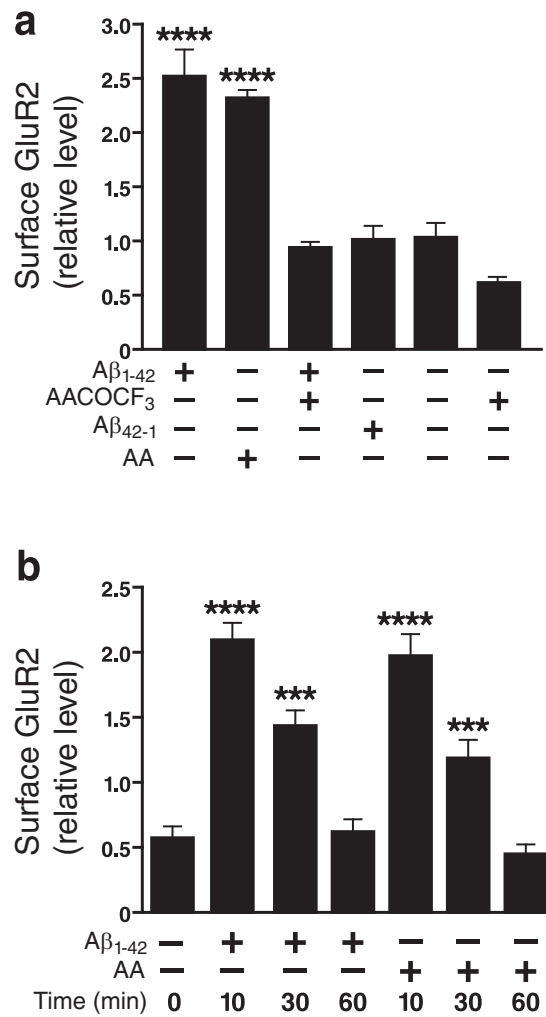
## Supplementary Figure 8



**Supplementary Figure 8.** Regulation of Aβ-mediated GIVA-PLA<sub>2</sub> activation and neurotoxicity. **a**, Aβ<sub>1-42</sub> (10 μM) increased GIVA-PLA<sub>2</sub> phosphorylation, whereas cell-secreted hAPP (sAPP) had no effect. Aβ<sub>1-42</sub>-dependent GIVA-PLA<sub>2</sub> phosphorylation was blocked by inhibitors of MAPK (SB203580) or MEK (PD98059) (P<0.0001 by one-way ANOVA). n=3 wells per condition in each of four independent experiments. p-GIVA-PLA<sub>2</sub> levels were normalized to tubulin levels. **b**, Aβ<sub>1-42</sub>, but not sAPP, increased AA release. Neurons were preincubated with <sup>3</sup>H-AA 6 hours before treatments, and AA release was assessed 30 minutes after treatments. Aβ<sub>1-42</sub>-dependent AA release was blocked by Ca<sup>2+</sup> chelation (EGTA+BAPTA), GIVA-PLA<sub>2</sub> inhibition (AACOCF<sub>3</sub>), and kinase inhibitors (SB203580 and PD98059), but not by inhibition of GVIA-PLA<sub>2</sub> (BEL) (P<0.001 by one-way ANOVA). n=3 wells per condition in each of six independent experiments. **c**, Aβ<sub>1-42</sub>-induced death of cultured primary neurons was diminished by inhibitors of AMPAR (NBQX) or GIVA-PLA<sub>2</sub> (AACOCF<sub>3</sub>), but not by an inhibitor of GVIA-PLA<sub>2</sub> (BEL) (P<0.0001 by repeated-measures ANOVA). Pretreatment with NBQX was sufficient to reduce neuronal death at 6 hours after Aβ<sub>1-42</sub> exposure (P<0.0001 vs Aβ<sub>1-42</sub> by post-hoc Tukey test). NBQX also decreased AA-induced neurotoxicity (P<0.0001 vs AA by post-hoc Tukey). n=2 wells per condition in each of three independent experiments. \*\*\*P < 0.01, \*\*\*\*P < 0.0001 vs. Aβ<sub>42-1</sub> by post-hoc Tukey test (mean ± s.e.m.).

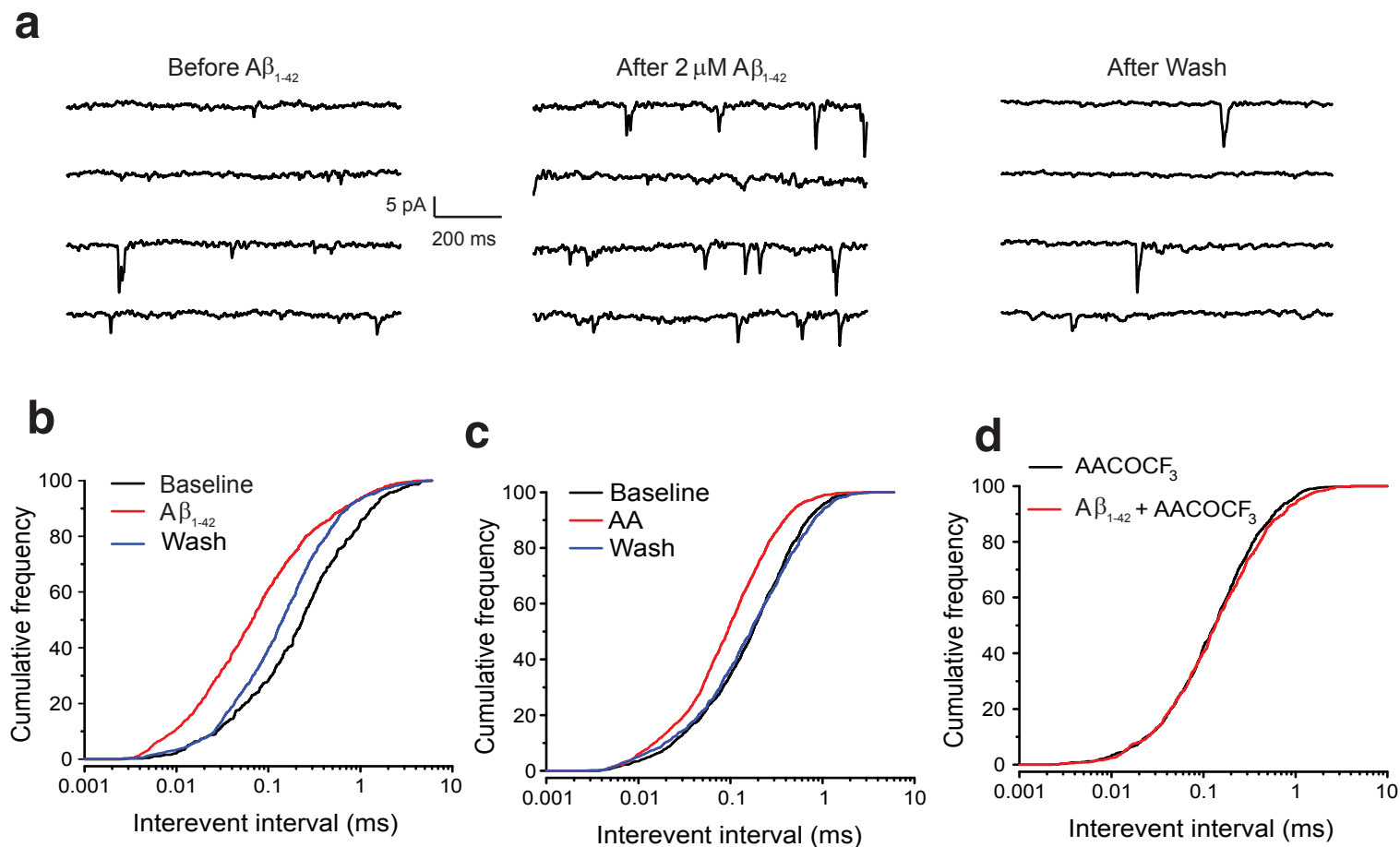


## Supplementary Figure 9



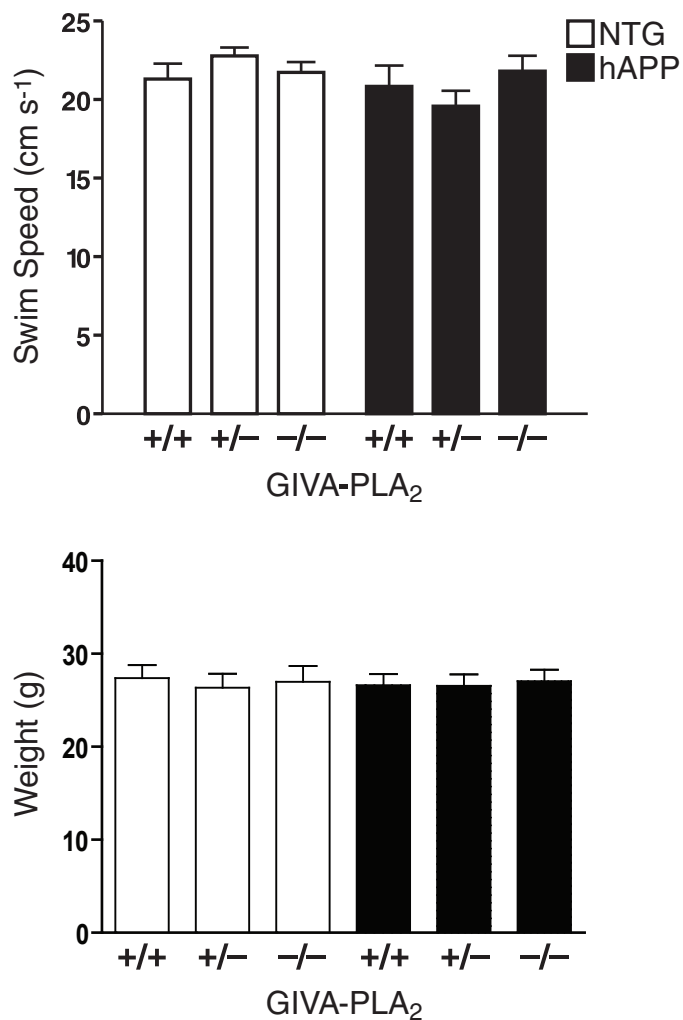
**Supplementary Figure 9.** Neuronal levels of surface GluR2 after Aβ and AA treatment. **a**, Surface levels of GluR2 were assessed by biotinylation assay 10 min after the indicated treatments. Treatment with Aβ<sub>1-42</sub> increased surface levels of GluR2 compared to Aβ<sub>42-1</sub>, an effect that could be blocked by inhibition of GIVA-PLA<sub>2</sub> (AACOCF<sub>3</sub>) and simulated with AA (mean ± s.e.m.). **b**, Surface levels of induced GluR2 decreased after 30 and 60 min of exposure to Aβ<sub>1-42</sub> or AA (mean ± s.e.m.). \*\*\*  $P < 0.001$ , \*\*\*\*  $P < 0.0001$  vs. Aβ<sub>42-1</sub> (a) or vs. time=0 (b) by post-hoc Tukey test. n=3 wells per condition in each of four independent experiments (mean ± s.e.m.).

## Supplementary Figure 10

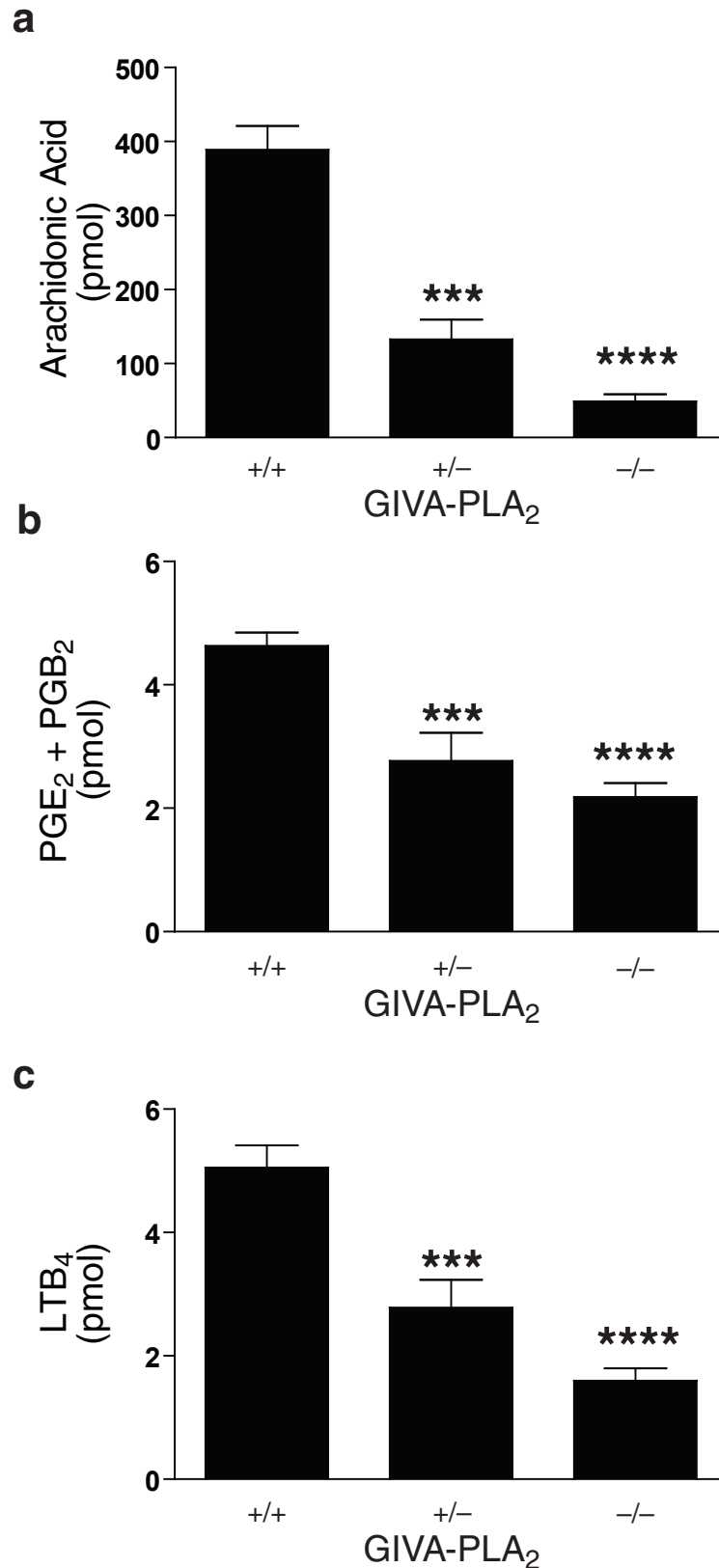


**Supplementary Figure 10.**  $A\beta_{1-42}$  effects on neuronal activity. Cortical slices were prepared from 4-month-old C57BL/6J NTG mice. Neuronal activity was recorded from layer 5 pyramidal neurons in the presence of GABA<sub>A</sub> (10  $\mu M$ ). **a**, Representative spontaneous (s) EPSC traces recorded from a single voltage-clamped neuron before (left) and 5 minutes after (middle) application of  $A\beta_{1-42}$  (2  $\mu M$ ), and 7 minutes after washout (right). For each condition, four segments of a continuous trace are shown. Note increased frequency of sEPSCs after the  $A\beta_{1-42}$  treatment. **b**, Cumulative histogram demonstrating that sEPSC interevent intervals were reversibly decreased by  $A\beta_{1-42}$  ( $P < 0.01$ ,  $n = 3$  neurons). **c**, AA had a similar effect ( $P < 0.01$ ,  $n = 5$  neurons). **d**, Inhibition of GIVA-PLA<sub>2</sub> (AACOCF<sub>3</sub>) blocked the  $A\beta_{1-42}$  effect ( $P > 0.20$ ,  $n = 3$  neurons). Statistics were performed by 2-sample Kolmogorov-Smirnov test with 3 minutes of data for each neuron.

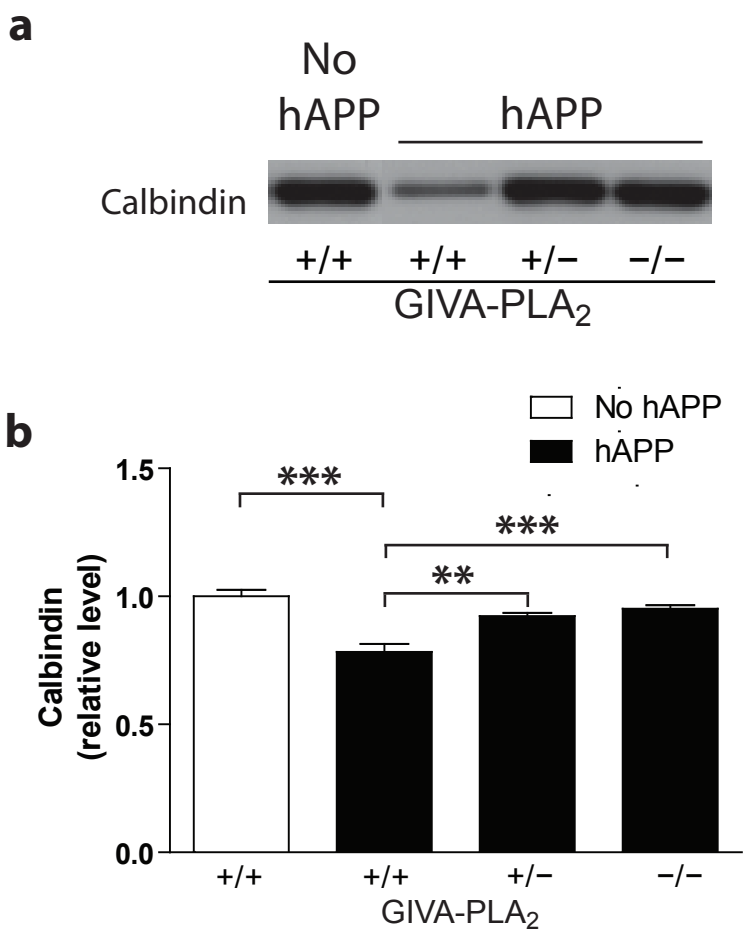
## Supplementary Figure 11



**Supplementary Figure 11.** GIVA-PLA<sub>2</sub>-deficient mice have normal swim speeds and body weights. Swim speeds determined during cued Morris water maze training did not differ among mice of the indicated genotypes. Body weights were also similar across genotypes. n=8–15 mice per genotype (mean ± s.e.m.); age, 4–6 months.

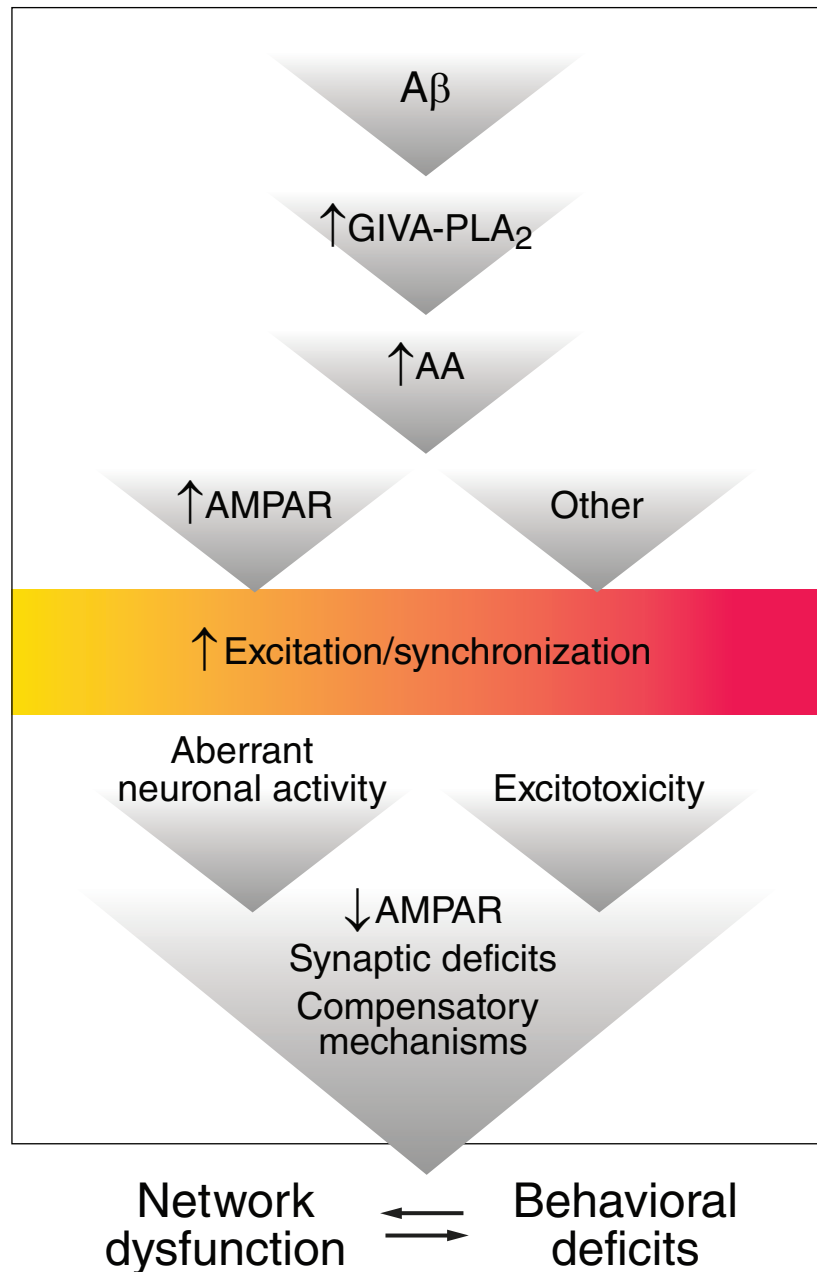


**Supplementary Figure 12.** Removal or reduction of GIVA-PLA<sub>2</sub> in hAPP mice reduced hippocampal levels of AA, PGE<sub>2</sub> + PGB<sub>2</sub>, and LTB<sub>4</sub>. \*\*\*P<0.001, \*\*\*\*P<0.0001 vs. GIVA-PLA<sub>2</sub> wildtype by post-hoc Tukey test. Fatty acid levels normalized to mg of total protein in sample. n = 4–6 mice per genotype (mean ± s.e.m.); age, 4 months.



**Supplementary Figure 13.** GIVA-PLA<sub>2</sub> reduction prevents neuronal calbindin depletion in hAPP mice. Representative western blot showing calbindin-D<sub>28K</sub> levels in the dentate gyrus of mice with the indicated genotypes. **b**, Densitometric quantitation of western blot signals revealed that GIVA-PLA<sub>2</sub> reduction prevented the hAPP/A $\beta$ -dependent reduction of calbindin-D<sub>28K</sub>. \*\*P<0.01, \*\*\*P<0.001 by post-hoc Tukey test. Calbindin levels normalized to tubulin levels. n= 7–9 mice per genotype (mean  $\pm$  s.e.m.); age, 6 months.

## Supplementary Figure 14



**Supplementary Figure 14.** Potential role for GIVA-PLA<sub>2</sub> in Aβ-mediated neuronal deficits. Oligomeric Aβ activates GIVA-PLA<sub>2</sub>, leading to the generation of AA and its metabolites. AA can increase AMPAR activity, presumably by blocking phosphorylation of GluR2 receptors by PKC, resulting in higher surface AMPAR levels, which increase neuronal excitability. When excessive, neuronal excitation can cause neurotoxicity or aberrant neural network activity. Together, aberrant neuronal activity, excitotoxicity, and compensatory mechanisms can decrease AMPAR and cause synaptic deficits, network dysfunction, and behavioral deficits that may be ameliorated by removal or reduction of GIVA-PLA<sub>2</sub>.